

# Nucleate and transition boiling in narrow horizontal spaces

Benoit Stutz · Monique Lallemand ·  
Fabien Raimbault · Julio Passos

Received: 22 August 2006 / Accepted: 9 May 2007 / Published online: 28 August 2007  
© Springer-Verlag 2007

**Abstract** Nucleate and transition boiling are performed in a horizontal narrow space between a heated upward-facing copper disk and an unheated surface for saturated *n*-pentane. The heat flux and the wall temperature are determined by mean of an inverse heat conduction method. The influence of the confinement on the boiling curves and the flow patterns are analysed. Characteristic instabilities are observed at low heat flux and during the transition regime.

## Latin symbols

<i>Bo</i>	Bond number
<i>C<sub>sf</sub></i>	coefficient in the Rohsenow correlation
<i>D</i>	diameter (m)
<i>f</i>	frequency (Hz)
<i>g</i>	acceleration of gravity ( $\text{m s}^{-2}$ )
<i>h<sub>lv</sub></i>	latent heat of vaporization ( $\text{J kg}^{-1}$ )
<i>k</i>	coefficient in the Haramura–Katto correlation
<i>L<sub>cap</sub></i>	capillary length (m)
<i>p</i>	pressure ( $\text{N m}^{-2}$ )
$\dot{q}$	heat flux ( $\text{W m}^{-2}$ )
$\dot{q}_{\text{crit}}$	critical heat flux ( $\text{W m}^{-2}$ )
<i>r<sub>c</sub></i>	cavity radius (m)
Ra	roughness (m)
<i>s</i>	gap size (m)

<i>t</i>	time (s)
<i>T</i>	temperature (K)

## Greek symbols

$\Delta T_{\text{sat}}$	wall superheat $\Delta T_{\text{sat}} = T_w - T_{\text{sat}}$ (K)
$\lambda$	conductivity ( $\text{W m}^{-1} \text{K}^{-1}$ )
$\rho$	density ( $\text{Kg m}^{-3}$ )
$\sigma$	surface tension ( $\text{N m}^{-1}$ )

## Subscripts

imp	imposed
l	liquid
ONB	onset boiling
s	relative to the confined space
sat	saturated conditions
v	vapour
w	wall
z	predicted by Zuber's model

## 1 Introduction

Boiling in narrow spaces occurs in many practical situations such as electronic component cooling, micro heat exchangers, engine cooling or steam generators, and has received substantial attention in the past. Compared with unconfined pool boiling, confinement improves heat transfer at low heat flux but reduces heat transfer at high heat flux [1]. The alternate drying and wetting of the heated surface associated with chemical concentration in confined space can be at the origin of corrosion problems [2]. Pool boiling in confined vertical spaces (annular or rectangular) and force convective boiling in confined space has been the subject of many researches considering the industrial applications. Conversely the existing literature concerning nucleate boiling in narrow horizontal spaces is limited.

B. Stutz (✉) · M. Lallemand · F. Raimbault  
CETHIL, UMR5008, CNRS, INSA-Lyon,  
Université Lyon1, F69621 Villeurbanne, France  
e-mail: benoit.stutz@insa-lyon.fr

J. Passos  
LABSOLAR-CNTS, Universidade Federal de Santa Catarina,  
Florianopolis, SC, Brazil

Katto and Yokoya [3] and Katto et al. [4] investigated nucleate pool boiling in a narrow space between two horizontal parallel disk-surfaces for saturated water at atmospheric pressure. It was found that keeping the heat flux constant, the wall temperature is invariable while the confinement plate is located apart from the heated surface. It falls as the gap size becomes smaller than the bubble detachment diameter and rises when the gap size is reduced further. Boulanger et al. [5] studied saturated nucleate boiling of pure R-113, water and mixtures of water/ethylene-glycol on a single nucleation site in a confined space for vertical and horizontal orientations. For pure components, confinement enhances heat transfer since deformation of bubbles leads to the broadening of their micro-layer. For the same experimental configuration Lallemand et al. [6] observed higher heat transfer coefficients for mixtures of binary water/ethylene-glycol than for pure water in confined configurations because of the change in some fluid properties implying a decrease in the bubble diameter. The mass diffusion process and the increase of the fluid viscosity are considered as beneficial phenomenon to limit heat transfer deterioration at high heat flux. Passos et al. [7] performed experiments for saturated FC72 and FC87 and subcooled nucleate pool boiling on a downward facing surface and in confined spaces between a heated copper disk and an unheated surface. For subcooled conditions, they observed that the effect of the confinement is opposite to that for saturated boiling (an increase in the confinement cause a reduction in the heat transfer coefficient).

The purpose of this work is to describe nucleate and transition boiling in a horizontal narrow space between a heated upward-facing copper disk and an unheated surface placed parallel to the heated surface for saturated *n*-pentane. At least, the objective is to establish a large database for pool boiling heat transfer in horizontal narrow spaces with various working fluids and various geometrical configurations (size of the heating surface, upward facing or downward-facing of the heated surface, ...) in order to better understand the different mechanisms involved in nucleate and transition boiling in narrow horizontal spaces.

## 2 Experimental set-up and procedure

### 2.1 Experimental set-up

A schematic diagram of the experimental device is shown in Fig. 1. The pool-boiling vessel is a 160 mm inner diameter and 150 mm height cylinder. The experiments are performed using pentane as test liquid in saturated conditions at  $p = 1$  bar ( $T_{\text{sat}} = 36^\circ\text{C}$ ). The capillary length is close to  $L_{\text{cap}} = 1.6$  mm. The pressure is maintained constant during the experiments using an external condenser

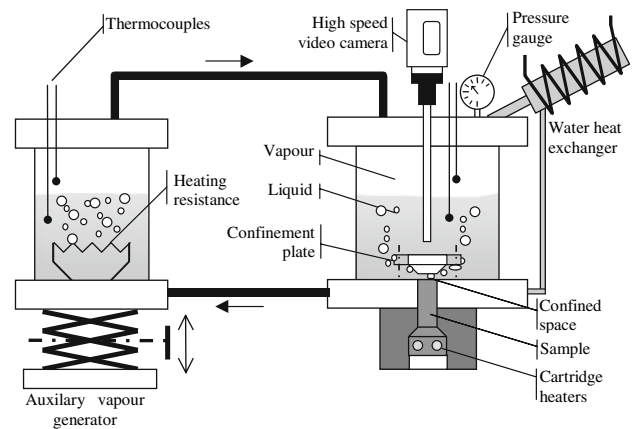


Fig. 1 Experimental set-up

and a vapour generator. The test heater is a 90 mm height cylindrical copper block, isolated on its perimeter with Teflon<sup>®</sup> ( $\lambda = 0.25 \text{ W m}^{-1} \text{ K}^{-1}$ ). Two cartridge heaters are imbedded in the sample. The 30 mm diameter-boiling wall is horizontal and mounted flushed with the vessel bottom. The surface is polished using a 600-grid emery paper. Roughness characteristics of the heater surface have a Ra value of 1  $\mu\text{m}$ . Two chromel-alumel thermocouples located at 12.2 and 47.6 mm beneath the surface are used to determine the heat flux and the wall temperature by means of an inverse heat conduction method [8]. Uncertainty of the wall temperature due to the uncertainties in the thermocouple position, copper thermal properties and thermocouple calibration is around  $\pm 0.2$  K. The accuracy in surface heat flux is within  $\pm 0.2 \text{ W cm}^{-2}$  for heat flux smaller than  $5 \text{ W cm}^{-2}$  and within  $\pm 0.5 \text{ W cm}^{-2}$  for higher heat flux. The data acquisition rate and thus the calculation rate of the surface heat flux and surface temperature superheat is 1 Hz. The free level of pentane is held at approximately 90 mm above the heating surface.

A conical unheated Plexiglas<sup>®</sup> plate ( $\lambda = 0.18 \text{ W m}^{-1} \text{ K}^{-1}$ ) is placed parallel to the heating surface ( $45^\circ$  cone angle; 30 mm diameter at bottom) (Fig. 2). It permits observations of the behaviour of the vapour and liquid in

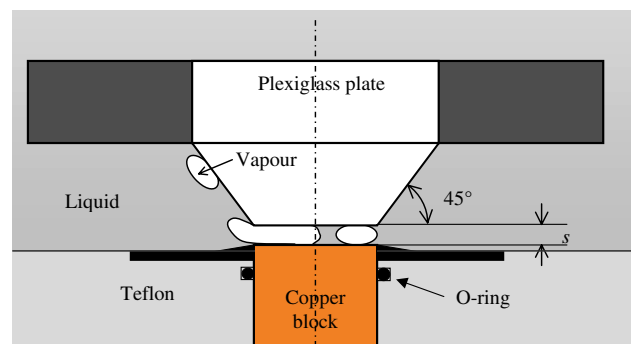


Fig. 2 Detail of the confinement plate

the confinement space using an endoscope associated with a high-speed video camera ( $250 \text{ frame s}^{-1}$ ). The gap size ( $200 \mu\text{m} \leq s \leq 90 \text{ mm}$ ) is accurately set by means of an optical device. The error caused by thermal expansion is lower than  $0.01 \text{ mm}$ .

## 2.2 Experimental procedure

According to Duluc et al. [9] transient nucleate boiling regime can be considered as a quasi-static regime for thick flat samples except for fast transient responses that follow boiling incipience. During nucleate pool boiling, the bubble emission frequency increases with the wall superheat and is higher than 40 bubbles/s with pentane in saturated condition [10]. The temperature of the heating surface shows locally high amplitude variations (few degrees) over very short times (few micro-seconds) corresponding to the high heat transfer variations occurring during the waiting and the bubble growth periods. The depth of solid affected by such temperature oscillations does not exceed a few tenths of mm around the nucleation sites. Therefore boiling curves obtained in low transient condition merges with steady-state nucleate boiling curves. A transient procedure is applied to describe the boiling curve from the transition regime to the free natural convection regime by decreasing the heat flux. Figure 3 shows the time evolution of the wall superheat  $\Delta T_{\text{sat}}$ , the heat flux released to the liquid  $\dot{q}_w$  and the imposed heat flux  $\dot{q}_{\text{imp}}$  during the experimental procedure for non confined ( $s = 90 \text{ mm}$ ) and confined ( $s = 0.8 \text{ mm}$ ) conditions.

The imposed heat flux is first gradually supplied to the test heater. At early stages, heat transfer is performed by convection and cell movements can be observed in the fluid upon the heated surface. Boiling starts in a quasi-explosive manner (point A). Due to heat transfer enhancement associated with boiling occurrence, wall temperature decreases whereas heat flux at the wall  $\dot{q}_w$  increases. Depending on the slope of the heat flux imposed to the cartridge heaters, the confinement and the superheat at boiling incipience, nucleate boiling develops or not over the whole heated surface before describing the transient regime. In the non-confined case plotted on Fig. 3a, the heat flux transferred to the fluid overcomes momentarily the heat flux imposed at the base of the test heater just after the boiling incipience. Afterward the upper part of the boiling curve corresponding to the nucleate boiling is plotted by increasing heat flux and the critical heat flux is reached (point B). When the superheat of the heating surface increases further, the boiling regime enters the transition region. Heat transfer degrades, wall temperature increases whereas heat transfer to the liquid decreases ( $d\dot{q}_w/d\Delta T_{\text{sat}} < 0$ ). In the confined case plotted on Fig. 3b,

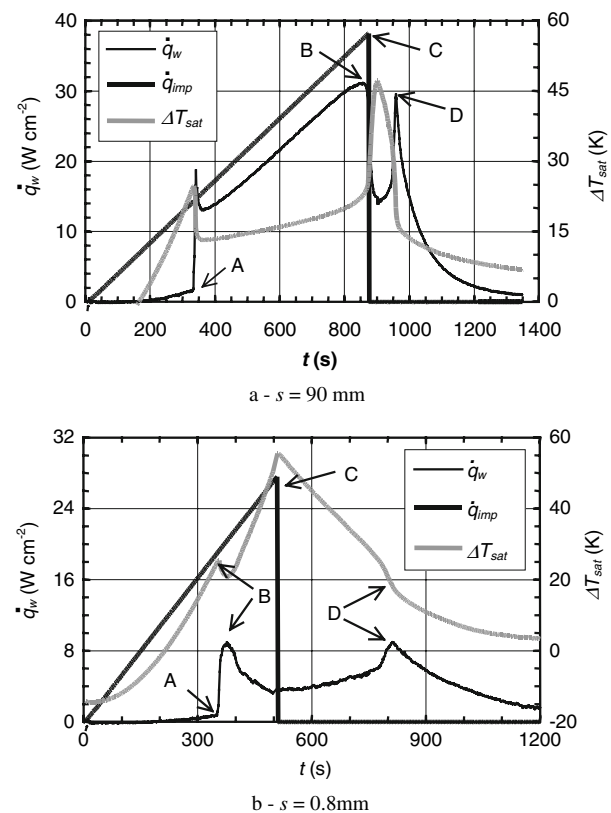


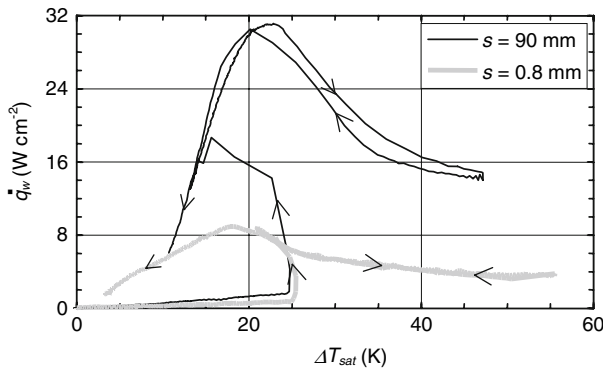
**Fig. 3** Time evolution of the heat flux released to the liquid and the wall superheat during the experimental procedure. **a**  $s = 90 \text{ mm}$  and **b**  $s = 0.8 \text{ mm}$

the transition boiling regime is achieved just after the boiling incipience.

Heat flux supplied to the test heater is switched off when the temperature becomes too high (point C). The Leidenfrost temperature  $\Delta T_{\text{Leidenfrost}} = 132 \text{ K}$  [11] has never been reached in the present experiments. The energy stored in the sample is released into the liquid. The temperature of the heated surface reached a maximum and starts to decrease. The boiling curve is then described by decreasing the surface temperature in transient condition: transition boiling, critical heat flux (point D), nucleate boiling and free convection.

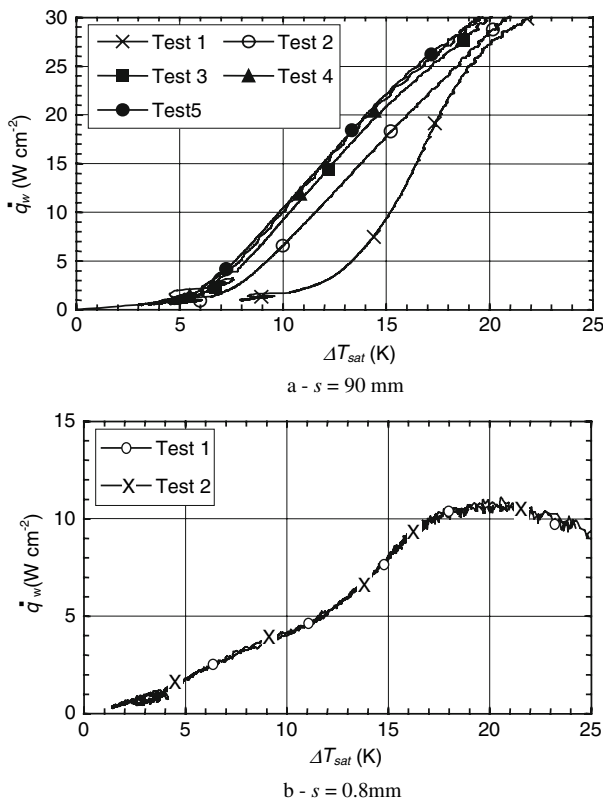
Figure 4 shows the boiling curves corresponding to the experimental runs presented in Fig. 3. During the transition regime, when the gap size is higher than the capillary length, boiling curves plotted by increasing and decreasing the surface temperature are different (for a given heat flux, heat transfer are higher when the boiling curve is described by increasing the surface temperature). When the gap size is smaller than the capillary length, boiling curves plotted by increasing and decreasing the surface temperature does not show any hysteresis effect except at boiling incipience.

Figure 5 shows successive boiling curves plotted after the polishing of the surface and the filling of the boiling



**Fig. 4** Boiling curves corresponding to the experimental runs presented in Fig. 3

vessel. When the gap size between the narrow horizontal plates is higher than the capillary length, boiling curves shift to the left during the first test and converge to a very reproducible curve (Fig. 5a). The reproducibility of the boiling curves is immediate when the gap size between the narrow horizontal plates is smaller than the capillary length (Fig. 5b). In such conditions, heat transfers are less influenced by the nucleation conditions at the heating surface whereas heat transfer depends on the nucleation site density for pool boiling. To ensure reliable comparison boiling



**Fig. 5** Initial boiling curves plotted the polishing of the surface and the filling of the boiling vessel. **a**  $s = 90$  mm and **b**  $s = 0.8$  mm

curves are reproduced for each experimental condition until a high level of reproducibility is obtained.

### 3 Results

Figure 6 shows the influence of the confinement on the boiling curves. For unconfined boiling configuration ( $s = 90$  mm), the classical Rohsenow correlation with  $C_{sf} = 0.0055$ , used to predict the average heat transfer coefficient in the case of nucleate pool boiling induced by an horizontal plate facing upwards, is relevant with our experimental results. The experimental critical heat flux is equal to  $31.5 \text{ W cm}^{-2}$ . This is in agreement with the critical heat flux of  $28.5 \text{ W cm}^{-2}$  deduced from the Haramura and Katto model [12] for upward-facing horizontal small disk:

$$\dot{q}_{crit} = \dot{q}_{crit-z}(1+k)^{5/16} \left\{ \frac{\left[ 2\pi 3^{1/2} \left( \frac{\sigma}{g(\rho_l - \rho_v)} \right)^{1/2} \right]^2}{\frac{\pi}{4} D^2} \right\}^{1/16} \tag{1}$$

$k$  is an empirical constant ( $k = 0.83$ ),  $\dot{q}_{crit-z}$  is the critical heat flux predicted by the Zuber’s model.

$$\dot{q}_{crit-z} = 0,131 \rho_v h_{lv} (\sigma g (\rho_l - \rho_v) / \rho_v^2)^{1/4} \tag{2}$$

When the confinement plate is placed parallel to the heating plate, the critical heat flux decreases  $\dot{q}_{crit-s}$  with decreasing the gap size. The Leidenfrost temperature  $\Delta T_{Leidenfrost} = 132 \text{ K}$  [11] has never been reached in the present experiments.

The squeezing effect of the confinement on the bubbles is characterized by the Bond number  $Bo$ , ratio of the gap

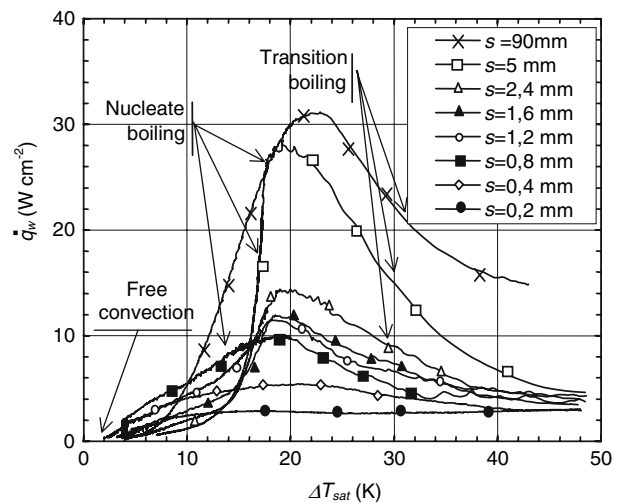


**Fig. 6** Boiling curves

size of the confinement space  $s$  to the capillary length  $L_{\text{cap}} = \sqrt{\sigma/g(\rho_l - \rho_v)} = 1.6$  mm. When  $Bo$  is greater than unity, the confinement wall does not deform the bubbles. The presence of the confinement plate prevents the formation of convection cell, disturbs the evacuation of the vapour phase leading to a deterioration of heat transfer: the heat transfer improvement induced by boiling in comparison with free convection is no more significant during the isolated bubble regime but remains quite important during the coalesced regime (although it is lower than without confinement). The ascensional velocity of bubbles and thus the micro-convection effects are reduced. When the Bond number is lower than unity, bubbles are squashed between the heated wall and the confinement plate during their growth. The evaporation of the thin liquid film formed between the squeezed bubbles and the heating wall leads to the improvement in heat transfer at low heat flux [4] and a change in the concavity of the boiling curves is observed. Unsteady behaviour corresponding to the onset and the disappearance of boiling within the confined space is observed at low heat flux; it is characterised by very low frequencies ( $f \approx 0.01$  Hz) (Fig. 7). Large nucleation sites are activated for wall superheat close to 4 K. Their diameter can be estimated using the following relation [13]:

$$r_c = \frac{2\sigma T_w}{\rho_v h_{lv} \Delta T_{\text{ONB}}} = 1.85 \mu\text{m}. \quad (3)$$

Onset of boiling is accompanied by heat transfer increase and thus a reduction of the heating surface temperature (Fig. 7). When the wall superheat becomes smaller than 3 K, the nucleation sites are deactivated and boiling stops, heat transfer decreases and heated surface temperature increases. Boiling starts again when the superheat reaches 4 K.

Visual investigations using high-speed video camera enable to describe the boiling regimes (Fig. 8). At low heat flux ( $\dot{q}_w/\dot{q}_{\text{crit}-s} < 0.2$ ), isolated bubbles appear on the

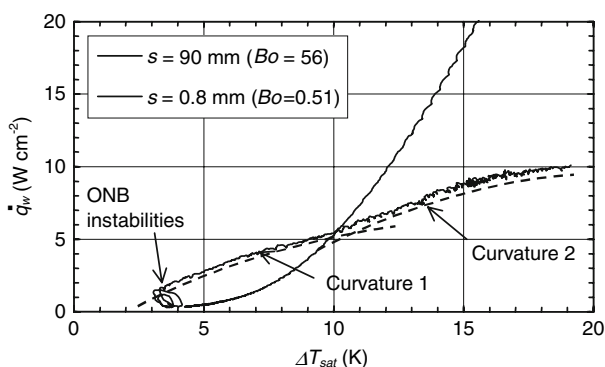


Fig. 7 Boiling curves for  $s = 0.8$  mm

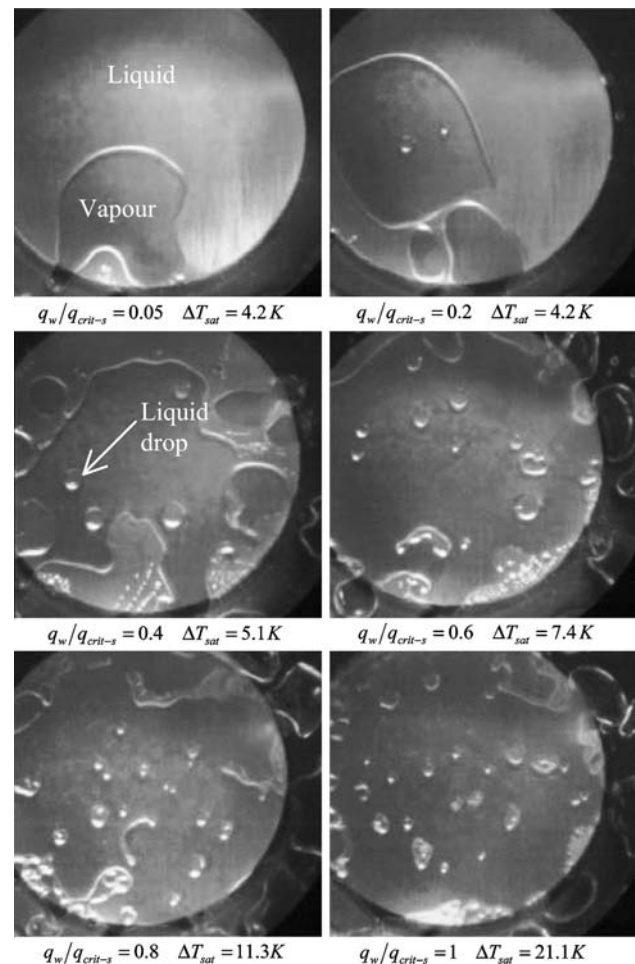


Fig. 8 Visualisation of nucleate boiling in a narrow space ( $s = 0.4$  mm)

heating surface. They grow and coalesce within the confined space. Bubbles escape at relatively low speed from the confined space. Liquid penetrates and fills the volume of escaping bubbles. Void fraction increases with increasing heat flux and boiling becomes more and more agitated. Liquid drops are wedged within the squeezed bubble during the coalescence processes ( $\dot{q}_w/\dot{q}_{\text{crit}-s} = 0.4$ ). For high heat fluxes ( $\dot{q}_w/\dot{q}_{\text{crit}-s} > 0.5$ ), boiling is characterized by violent liquid feeding and ejection from the confined space. Nucleation occurs very rapidly within the liquid during its re-entry. Bubbles almost do not exist anymore. Drops shapes are no more circular and typical “filament” can be observed on the heating surface. Analysis of the boiling curves corresponding to the nucleate boiling regime shows an inflexion point that can be explained by this change in the two-phase flow pattern (bubble flow for  $\dot{q}_w/\dot{q}_{\text{crit}-s} < 0.5$ ; agitated drop flow for  $\dot{q}_w/\dot{q}_{\text{crit}-s} > 0.5$ ) (Fig. 7).

The critical heat flux decreases with decreasing the gap size (Fig. 6). The temperature of the wall superheat corresponding to the critical heat flux is about 23 K for pool



boiling. It decreases when the confinement plate disturbs the evacuation of the vapour phase and becomes quite constant and equal to 18 K for Bond numbers included between 3.2 and 0.26. The notion of critical heat flux disappears when the gap size becomes too small (about 0.2 mm in the present case): burnout does not take place in a clear-cut manner anymore.

Figure 9 shows the evolution of the critical heat flux as a function of the gap size  $s$ . A significant change appears when  $s$  reaches a value closed to the capillary length  $L_{\text{cap}}$ . The same tendency was previously pointed out by Katto et al. [4] for saturated water boiling between two horizontal disk surfaces (11 mm in diameter). At high heat fluxes, when the gap size is greater than the capillary length, the heated surface is wetted with a liquid film, which includes numerous columnar vapour steams. The vapour generated accumulates to form massive vapour bubbles that rise away regularly from the liquid film. The critical heat flux occurs when the time required for the liquid film to dry out becomes smaller than the hovering period of the massive vapour bubbles. The effect of the confinement plate is to degrade the conditions of the massive vapour blanket emission. The gap size reduction leads to the increase of the hovering period of the massive vapour bubbles and thus to the reduction of the critical heat flux.

When the gap size is smaller than the capillary length, the mechanisms are different: when the heat flux is higher than  $0.5 \dot{q}_w / \dot{q}_{\text{crit}-s}$ , dry portions, liquid films and agitated drops coexist on the heated surface. The transition regime occurs when the feeding of liquid becomes insufficient to cool the heated surface but the mechanisms do not differ significantly in comparison with the nucleate boiling regime.

During the transition boiling, heat transfers are transient and a steady state cannot be achieved because of the inertia of the heated sample and the slope of the boiling curve. The boiling curves plotted by decreasing or increasing heat flux are similar (no significant hysteresis effect has been

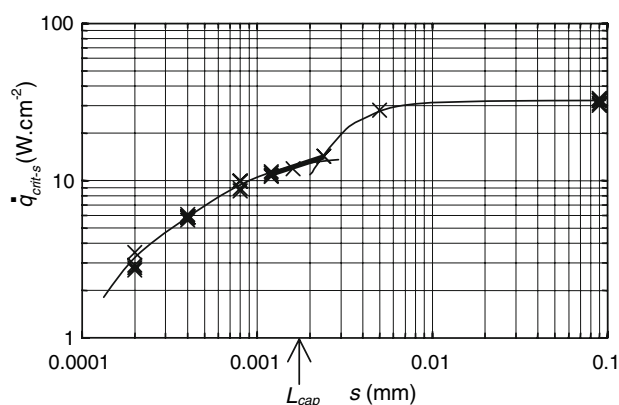


Fig. 9 Evolution of the critical heat flux with the gap size

observed). Their shapes are similar to the one mentioned in the literature and obtained by imposing the temperature of the heating wall. The curves obtained in confined conditions seem to converge to a same point (Fig. 6). The high-speed video films show the presence of a thin liquid film along the confinement plate. When the liquid makes contact with the dry heated wall, intense nucleate boiling takes place and fine liquid drops are scattered around (Fig. 10). The high velocity of the vapour phase destabilized the liquid film (Kelvin Helmholtz instabilities) and characteristic capillary waves can be observed using high-speed video camera. The liquid contact between the liquid film developing along the confinement plate and the dry heated wall occurs regularly. The frequency of the phenomenon is close to 15 Hz.

#### 4 Conclusion

This paper concerns nucleate boiling and transition boiling in a horizontal narrow space between a heated upward-facing copper disk and an unheated plate placed parallel to the heated wall for saturated n-pentane.

The presence of the confinement plate affects heat transfer. When the Bond number is greater than unity, the heat transfer improvement induced by boiling in comparison with free convection is no more significant during the isolated bubble regime but remains quite important during the coalesced regime. When the Bond number is lower than unity, heat transfers are enhanced at low heat flux. This improvement is attributed to the evaporation of the thin liquid film formed between the squeezed bubbles and the heating wall. The apparition of boiling agitation ( $\dot{q}_w / \dot{q}_{\text{crit}-s} > 0.5$ ) lead to additional heat transfer increase.

Characteristic instabilities are observed at low heat flux and correspond to the onset and the disappearance of

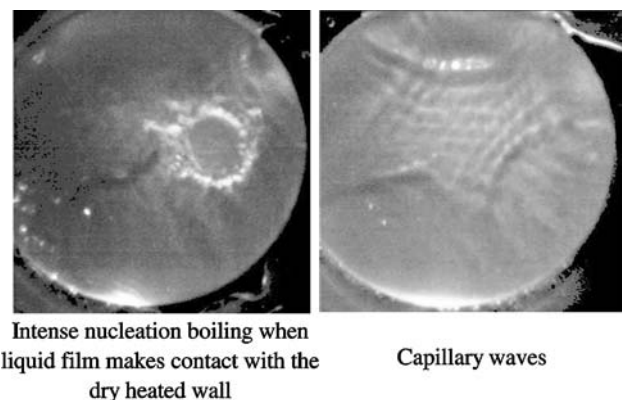


Fig. 10 Visualisation of transition boiling in a narrow space ( $s = 0.4$  mm). **a** Intense nucleation boiling when liquid film makes contact with the dry heated wall and **b** capillary waves

boiling ( $f = 0.01$  Hz). At high heat flux the thin liquid film that develops along the confinement plate makes regularly contact with the dry heated surface with a frequency is close to 15 Hz.

The reduction of the critical heat flux with the gap size decreases when the confinement space becomes lower than the capillary length. In that case, the mechanisms involved in heat transfer do not differ significantly during transition boiling and nucleate boiling.

## References

1. Bonjour J, Lallemand M (1998) Flow patterns during boiling in a narrow space between two vertical surfaces. *Int J Multiph Flow* 24:947–960
2. Hung YH, Yao SH (1985) Pool boiling heat transfer in narrow horizontal annular crevices. *Trans ASME J Heat Transf* 107:656–662
3. Katto Y, Yokoya S (1966) Experimental study of nucleate pool-boiling in case of making interference-plate approach to the heating surface. In: *Proceedings of 3rd Int. J. Heat Transfer Conf, Chicago*, pp 219–227
4. Katto Y, Yokoya S, Terakoa K (1977) Nucleate and transition boiling in a narrow space between two horizontal parallel disk-surfaces. *Bull JSME* 20:638–643
5. Boulanger F, Gentile D, Bonjour J, Lallemand M (1997) Heat transfer in a confined space and nucleation on a single site. *Int. symp. the physics of heat transfer in boiling and condensation, Moscow*, pp 381–385
6. Lallemand M, Bonjour J, Gentile D, Boulanger F (1998) The physical mechanisms involved in the boiling of mixtures in narrow spaces. *Int. Heat Transfer Conference, Kyongjiu, Korea*, pp 515–519
7. Passos JC, Hirata FR, Possamai LFB, Balsamo M, Misale M (2004) Confined boiling of FC72 and FC87 on a downward facing heating copper disk. *Int J Heat Fluid Flow* 25:313–319
8. Raynaud M (1992) Influence of convection on the boiling curves of liquid nitrogen estimated around the periphery of a rotating disk. In: *Proceedings of the Third UK National Conference, Incorporating 1st European Conference on Thermal Science, ETS*, pp 147–153
9. Duluc MC, Stutz B, Lallemand M (2004) Transient nucleate boiling under stepwise heat generation for highly wetting fluids. *Int J Heat Mass Transfer* 47:5541–5553
10. Cusursuz A, Ginet N, Cioulachtjian S, Lallemand M (2001) Durée d'attente, durée de grossissement d'une bulle isolée, *Congrès français de thermique, Nantes*, 6p
11. Carey VP (1992) *Liquid-vapour phase change phenomena*. Taylor & Francis, Philadelphia
12. Haramura Y, Katto Y (1983) A new hydrodynamic model of critical heat flux, applicable widely to both pool and forced convection boiling on submerged bodies in saturated liquids. *Int J Heat Mass Transfer* 26:389–399
13. Griffith P, Wallis J (1960) The role of surface condition in nucleate boiling. *Chem. Eng. Prog. Symp.*, pp 49–63